HHS Public Access

Author manuscript

ACS Chem Neurosci. Author manuscript; available in PMC 2023 February 01.

Published in final edited form as:

ACS Chem Neurosci. 2021 January 06; 12(1): 234–243. doi:10.1021/acschemneuro.0c00711.

Characterization of kinetic isotope effects and label loss in deuterium-based isotopic labeling studies

Robin A. de Graaf,

Monique A. Thomas,

Kevin L. Behar,

Henk M. De Feyter

Departments of Radiology and Biomedical Imaging, Magnetic Resonance Research Center, Yale University School of Medicine, New Haven, Connecticut, USA

Abstract

Deuterium metabolic imaging (DMI) is a novel, 3D, magnetic resonance (MR)-based method to map metabolism of deuterated substrates *in vivo*. The replacement of protons with deuterons could potentially lead to kinetic isotope effects (KIEs) in which metabolic rates of deuterated substrates are reduced due to the presence of a heavier isotope. Knowledge of the extent of KIE *in vivo*, and ^{2}H label losses due to exchange reactions is required for DMI-based measurements of absolute metabolic rates. Here the deuterium KIE and label loss *in vivo* is investigated for glucose and acetate using a double substrate/double labeling strategy and ^{1}H-decoupled ^{13}C NMR in rat glioma cells and rat brain tissue metabolite extracts. The unique spectral patterns due to extensive ^{2}H-^{13}C and ^{13}C-^{13}C scalar coupling allows the identification of all possible metabolic products. The ^{2}H label loss observed in lactate, glutamate and glutamine of rat brain were 15.7 ± 2.6, 37.9 ± 1.1 and 41.5 ± 5.2 % when using [6,6-$^{2}H_2$]-glucose as the metabolic substrate. For [2-$^{2}H_3$]-acetate, the ^{2}H label losses in glutamate and glutamine were 14.4 ± 3.4 and 13.6 ± 2.2 %, respectively, in excellent agreement with predicted values. Steady-state ^{2}H label accumulation in the C4 position of glutamate and glutamine was contrasted by the absence of label accumulation in the C2 or C3 positions, indicating that during a full turn of the tricarboxylic acid cycle all ^{2}H label is lost. The measured KIE was relatively small (4–6%) for both substrates, and all measured metabolic products. These results pave the way for further development of quantitative DMI studies to generate metabolic flux maps *in vivo*.

Graphical Abstract

Address correspondence to: Robin A. de Graaf, Ph.D., Magnetic Resonance Research Center, Department of Radiology and Biomedical Imaging, Yale University School of Medicine, 300 Cedar Street, P.O. Box 208043, New Haven, CT 06520-8043, USA. Tel: (203) 785-6203, Fax: (203) 785-6643, robin.degraaf@yale.edu.

Author Contributions

RAdG: study design, data acquisition and processing, writing; MAT, experiments, tissue processing; KLB: study design, writing; HMDF: study design, data acquisition, writing.

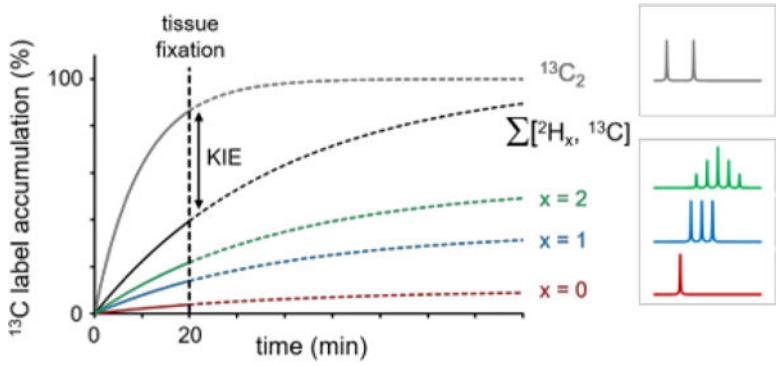

Keywords

deuterium; kinetic isotope effect; label loss; glucose; acetate

INTRODUCTION

Stable isotope labeling strategies are abundantly used in the study of intermediary metabolism *in vitro* and *in vivo*. Since carbon forms the backbone of many biologically relevant compounds, carbon-13 (^{13}C) is a commonly used isotope. When combined with ^{13}C MR spectroscopy (MRS), a wide range of ^{13}C-labeled substrates and metabolic products can be detected based on differences in chemical shift and scalar coupling patterns. ^{13}C MRS has been used in combination with intravenous infusion of ^{13}C-labeled substrates to study the relationship between energy metabolism and neurotransmission in the human and animal brain *in vivo* [1,2], study glycogen synthesis in muscle and liver *in vivo* [3,4] and characterize brain tumor metabolism [5–7].

Other stable isotopes that are used *in vivo* to study metabolism are deuterium (^{2}H), nitrogen-15 (^{15}N) and oxygen-17 (^{17}O). The interest in deuterium has seen a recent increase in the field of MR-based metabolic imaging. In hyperpolarized ^{13}C MR studies, protons are replaced with deuterium in order to lengthen the ^{13}C T_1 relaxation time constant and hence the lifetime of the hyperpolarized state [8,9]. Deuterium itself is also a useful isotope to study intermediary metabolism as evidenced by the recently described deuterium MRS (DMS) and deuterium metabolic imaging (DMI) methods [10,11]. The relatively high MR sensitivity attributed to the favorable T_1 and T_2 relaxation times, and magnetic moment of ^{2}H allows the acquisition of 3D metabolic images of ^{2}H-labeled substrate metabolism [12]. In addition, the relatively simple ^{2}H acquisition methods that do not require water or lipid suppression, in combination with enhanced immunity to magnetic field inhomogeneity due to the low ^{2}H gyromagnetic ratio, make DMI a very robust metabolic imaging method.

As with any isotope labeling strategy, one needs to consider the presence of a kinetic isotope effect (KIE) by which the rate of a chemical reaction is decreased when one or more atoms of a reactant are replaced with a heavier isotope. The KIE for ^{13}C labeling strategies is generally small, due to the modest mass increase between ^{12}C and ^{13}C. The 100% mass increase from ^{1}H to ^{2}H isotope replacement can lead to significant KIEs [13] depending on the exact reaction mechanism [14]. To generate accurate maps of absolute metabolic rates *in vivo*

using DMI, the extent of potential KIE's of the deuterated substrate of interest needs to be known.

In addition to the KIE, which potentially applies to any isotope labeling method, ^{2}H labeling strategies can also be affected by ^{2}H label loss. Several chemical equilibrium reactions, such as keto-enol tautomerization, involve exchange between reactant protons and water protons. In the presence of ^{2}H labeling, these exchange reactions can lead to a partial replacement of ^{2}H by ^{1}H and therefore ^{2}H label loss. Knowledge of the fraction of ^{2}H label that is lost from a substrate of interest is required to accurately determine the concentration of ^{2}H-labeled metabolites detected *in vivo*.

Here we present a study on the KIE and label loss of deuterated glucose and acetate, commonly used substrates in MRS-based brain metabolism research *in vivo* [1]. Since a robust differentiation between KIE and ^{2}H label loss is not possible with ^{1}H or ^{2}H NMR methods, we employed ^{13}C NMR in combination with ^{13}C and ^{2}H double-labeled glucose and acetate. The ^{13}C chemical shifts and scalar coupling patterns provide a unique and unambiguous spectral fingerprint of the ^{2}H label loss and KIE of multiple brain metabolites, including lactate, glutamate and glutamine.

RESULTS and DISCUSSION

The use of ^{2}H as label to evaluate metabolic activity *in vivo* by ^{2}H MRS and DMI is increasingly gaining interest. For these techniques to be used in a quantitative manner it is critical to determine the extent of possible KIEs, and the extent of ^{2}H label loss of the ^{2}H-labeled metabolic substrates of interest. We investigated both the KIE and label loss for [6,6-$^{2}H_2$]-glucose and [$^{2}H_3$]-acetate, using a strategy that relies on co-administration of double-labeled substrates, both for *in vitro* and *in vivo* experiments. By combining both deuterated and protonated substrates each experiment is internally controlled for metabolic rate. This approach requires a method to distinguish both labeled and unlabeled substrates and/or products, such as NMR, although mass spectrometry can also be used as illustrated by Murphy et al. for the optimization of a PET imaging agent [15]. When keeping the total substrate dose constant the double-substrate approach leads to a two-fold reduction in the ^{13}C fractional enrichment compared to a single-substrate experiment. However, the ability to robustly detect small KIEs without intersubject variability outweighs the reduction in SNR.

Both KIEs and ^{2}H label loss result in a reduced amount of ^{2}H-label in downstream metabolites, which makes distinguishing KIEs from label loss challenging. We circumvented this problem by using deuterated and protonated substrates that were also labeled with ^{13}C (Fig. 1A). Since carbons reside in the backbone of the molecules, no exchange or loss of ^{13}C occurs, and potential KIEs from the presence of ^{13}C have been considered negligible *in vivo*. We strategically choose the protonated substrate to be doubly ^{13}C-labeled at two adjacent carbons, while the deuterated substrate contained a single ^{13}C. This approach relies on the assumption that ^{13}C KIEs -if not negligible- are identical for single ^{13}C and double $^{13}C_2$-labeled substrates and products. KIEs are typically most significant when a chemical bond involving the heavier isotope is broken (KIE of the first order) [14]. The ^{13}C-^{13}C chemical bond in [5, 6-$^{13}C_2$]-glucose and [1,2-$^{13}C_2$]-acetate is not broken until

the second turn of the TCA cycle, and therefore does not interfere with our approach. The peak splitting (doublet) due to ^{13}C-^{13}C J-coupling observed in a downstream metabolite is evidence of that metabolite originating from a doubly ^{13}C-labeled and thus protonated substrate. A metabolite that has lost all of its ^{2}H can still be traced back to its original deuterated substrate, because of the metabolite's appearance as a singlet in the ^{1}H-decoupled ^{13}C spectrum (Fig. 1C). When accounting for the small contribution of naturally abundant ^{13}C compounds, this strategy allows for accurately separating KIEs and ^{2}H label loss in downstream metabolites of the competing deuterated and protonated substrates (Fig. 1B).

Figure 2A shows a ^{13}C NMR spectrum of the C3 position of lactate in RG2 cell medium 6 hours following the co-administration of ^{13}C and ^{2}H-labeled glucose. The chemical shifts and splitting patterns indicate the presence of four distinct lactate species that can be quantitated through the use of spectral fitting. The presence of non-deuterated (red) and single-deuterated (blue) [3-^{13}C]-lactate in addition to double-deuterated [3-^{13}C]-lactate (green) indicates some degree of ^{2}H label loss in the glycolytic pathway. Figure 2B provides a quantitative summary of the [3-^{13}C]-lactate species formed from deuterated [6-^{13}C]-glucose. Non, single and double-deuterated lactate represent 3.2 ± 0.3 %, 20.7 ± 1.2 % and 76.1 ± 1.4 % (mean ± SD, n = 3) of all the lactate formed from deuterated glucose. For DMS and DMI studies, this ^{2}H label loss distribution would provide 86.4 ± 0.8 % of the maximum lactate signal intensity obtained in the absence of ^{2}H label loss. Figure 2C shows that the sum of lactate species produced from deuterated glucose represents 97.3 ± 0.9 % of the lactate produced from non-deuterated glucose ($p = 0.109$, Wilcoxon signed rank test).

Figure 3A shows the C4 chemical shift range of glutamate in rat brain extract following the co-administration of ^{13}C and ^{2}H-labeled glucose. Similar to ^{13}C-labeled lactate in Figure 2, the chemical shifts and scalar coupling patterns indicate the presence of four distinct glutamate species. The distribution of differently labeled lactate in rat brain closely mirrors the pattern shown in Figure 2A for lactate in RG2 cells. The spectral pattern for rat brain glutamine labeling resembles that of rat brain glutamate (Fig. 3A), albeit at circa three-fold lower intensity due to the smaller glutamine pool size. The visibly increased amounts of non-deuterated (red) and single-deuterated (blue) glutamate, and decreased amount of double-deuterated (green) glutamate relative to lactate indicate increased ^{2}H label loss along the metabolic pathway from lactate/pyruvate to glutamate. Figure 3B provides a quantitative description of the [$^{2}H_x$, 3-^{13}C]-lactate, [$^{2}H_x$, 4-^{13}C]-glutamate and [$^{2}H_x$, 4-^{13}C]-glutamine as formed from [6,6-$^{2}H_2$, 6-^{13}C]-glucose in rat brain. Non, single and double-deuterated lactate represent 6.1 ± 2.1 %, 19.2 ± 1.2 % and 74.7 ± 3.1 % (mean ± SD, n = 3) of all the lactate formed from deuterated glucose. The non, single and double-deuterated forms of ^{13}C-labeled glutamate represent 8.6 ± 0.9 %, 58.5 ± 1.0 % and 32.9 ± 1.5 % of all the glutamate originating from deuterated glucose. The distribution of ^{2}H label for glutamine is 17.1 ± 5.3 %, 48.9 ± 5.0 % and 34.0 ± 6.2 % for the non, single and double-deuterated forms. In DMS and DMI studies employing direct ^{2}H detection, these ^{2}H label distributions would lead to 84.3 ± 2.6 %, 62.1 ± 1.1 % and 58.5 ± 5.2 % signal intensity for lactate, glutamate and glutamine respectively, relative to signal in the theoretical absence of label loss. Alanine displayed a much greater level of ^{2}H label loss than lactate as judged by the large non-deuterated contribution (data not shown), consistent with the methyl group of alanine exchanging protons/deuterons with the environment during the aminotransferase

reaction [16]. The alanine ^{2}H label loss was not quantitatively pursued due to the low MR sensitivity. Figure 3C shows that the sum of ^{13}C-labeled lactate, glutamate and glutamine produced from deuterated glucose represents 96.0 ± 12.9 % ($p = 0.812$), 96.6 ± 6.2 % ($p = 0.018$) and 98.0 ± 19.3 % ($p = 0.406$) of the respective metabolites produced from non-deuterated glucose. In the classical description of KIE this equates to k_H/k_D ratios of 1.042, 1.035, and 1.020 for [6,6-$^{2}H_2$]-glucose metabolism resulting in labeling of lactate, glutamate and glutamine, respectively.

Figure 4A summarizes the ^{2}H label loss for glutamate and glutamine in rat brain following the administration of [$^{2}H_3$, 2-^{13}C]-acetate. Glutamate and glutamine have a very similar ^{2}H label distribution with the non, single and double-deuterated forms accounting for 1.9 ± 2.4 %, 25.0 ± 3.7 % and 73.1 ± 5.0 % of glutamate and 1.7 ± 2.7 %, 23.9 ± 1.9 % and 74.4 ± 2.1 % of glutamine. For direct ^{2}H-detected DMS and DMI studies, this ^{2}H label loss distribution would translate into 85.6 ± 3.4 % and 86.4 ± 2.2 % glutamate and glutamine signal intensity, respectively, relative to signal in the absence of label loss. Figure 4B shows that the sum of ^{13}C-labeled glutamate and glutamine produced from deuterated acetate represents 95.5 ± 9.6 % ($p = 0.045$, $k_H/k_D = 1.047$) and 94.1 ± 8.3 % ($p = 0.003$, $k_H/k_D = 1.063$) of the respective metabolites produced from non-deuterated acetate.

The infusion duration used for *in vivo* studies was 20 min, which represents a compromise between achieving sufficiently high (SNR) in the NMR spectra, and sensitivity to detection of KIEs. Using a longer infusion duration will result in higher SNR spectra due to higher levels of fractional enrichment, but being closer to isotopic steady state will reduce possible differences in isotopic labeling induced by KIEs (see also Fig.1B). A shorter than 20 min infusion time would be beneficial because less ^{13}C-labeling would occur from second-turn TCA cycle activity. The latter leads to ^{13}C label being redistributed to different carbon positions, which results in ^{13}C isotopomers. While ^{13}C isotopomer analysis is a very powerful method to study metabolism, it is typically applied after long infusion times, leading to steady state levels of labeling [17]. With a 20 min infusion the SNR of the ^{13}C signal representing second turn TCA activity was too low to be included in the analysis. The compromise between SNR and sensitivity for KIEs encountered in rat brain studies does not play a significant role during lactate detection in RG2 cancer cells. Lactate, produced as part of the linear glycolytic pathway, is transported to the cell culture medium where it accumulates. As a result, the lactate concentration increases over time, thereby improving the accuracy in determining both KIEs and ^{2}H label loss (Fig. S1).

The limited SNR is the result of relatively low levels of labeling due to the short duration of the *in vivo* experiments, but also because of the inherent low sensitivity of ^{13}C NMR. Standard methods to enhance the ^{13}C NMR sensitivity such as polarization transfer and nuclear Overhauser enhancement were not suitable for the current study as they enhance ^{13}C-^{1}H and ^{13}C-^{2}H species differently. This would require additional experiments to empirically measure the molecule-specific enhancement. Despite the differential effect on ^{13}C-^{1}H and ^{13}C-^{2}H species, proton decoupling was nevertheless employed. Firstly, proton decoupling greatly simplifies the appearance and enhances the sensitivity of ^{13}C NMR for ^{13}C-^{1}H species. Secondly, in the presence of ^{2}H label loss many ^{13}C-^{2}H species will contain one bond ^{13}C-^{1}H coupling (e.g. [3-^{2}H, 3-^{13}C]-lactate), and two and three-bond ^{13}C-^{1}H

scalar couplings are always present. Proton decoupling therefore also substantially improved the ^{13}C NMR spectrum of (partially) deuterated compounds. Deuterium decoupling, in addition to the applied proton decoupling, would lead to a substantial increase in SNR as the ^{13}C-$^{2}H_x$ multiplets collapse into singlets. The ability to differentiate various [$^{2}H_x$, ^{13}C]-labeled species would not be affected, as the presence of ^{2}H would shift the resonance frequency by 0.25 – 0.30 ppm per ^{2}H. Unfortunately, in the current study the application of simultaneous ^{1}H and ^{2}H decoupling was not practical, such that the ^{13}C MR spectra were acquired with ^{1}H decoupling only.

The described experiments have resulted in ^{2}H label loss correction factors that can be applied to *in vivo* brain metabolism studies using [6,6-$^{2}H_2$]-glucose or [$^{2}H_3$]-acetate (Table S2). The ^{2}H label loss observed between acetate and glutamate is caused by the aconitase-catalyzed dehydration of citrate into cis-aconitate and the subsequent hydration into iso-citrate. Due to the symmetry of citrate there is a 25% chance that a proton or deuteron is replaced by a water proton. This statistical prediction is in excellent agreement with the experimental data in which 73.1 ± 5.0 % of glutamate retains both deuterons and 25.0 ± 3.7 % of glutamate has lost a single deuteron. In addition to the aconitase-catalyzed dehydration/hydration reactions, the ^{2}H label loss observed between lactate and glutamate is affected by the conversion of acetyl-CoA into citrate by citrate synthase. The conversion of a methyl group in acetyl-CoA into a methylene group in citrate equates to a 2/3 or 66.7% statistical chance that a deuteron is passed from lactate to citrate. Given the ^{2}H distribution in lactate, the ^{2}H label accumulation in citrate can be predicted as 12.5 %, 37.7 % and 49.8 % for non, single and double-deuterated moieties, respectively. With the 25% chance of ^{2}H label loss between citrate and iso-citrate, the predicted ^{2}H label accumulation in glutamate is 21.9 %, 53.2 % and 24.9 % for non, single and double-deuterated moieties, respectively. The predicted values are in qualitative agreement with the experimental data.

Our studies were performed in rat tumor cells and brain tissue, but we anticipate that the label loss correction factors established here for [6,6-$^{2}H_2$]-glucose and [$^{2}H_3$]-acetate are applicable to other organs and mammals as well for the metabolic pathways we studied. The mechanisms of label loss and KIE are specific for the enzymatic reactions that constitute the metabolic pathways, and will need to be established for different substrates or for substrates labeled at different positions than tested here. In scenarios where ^{2}H label loss is suspected to be different than what is reported, and the extent of a KIE can be neglected, an experiment with a single substrate can provide the answer, and no double-label, double substrate is required. As long as a substrate is ^{13}C-labeled at the carbon atom that forms the bond with the deuteron(s), the degree of ^{2}H label loss can be determined in the downstream metabolite of interest using direct ^{13}C NMR. The presence or lack of chemical shifted species observed in the ^{13}C MR spectrum induced by bound ^{2}H represents the complete range of possible ^{2}H-labeled and unlabeled species. A number of previous publications have focused on ^{2}H label loss and KIEs in NMR studies of energy metabolism. Ben-Yoseph et al. used [6,6-$^{2}H_2$, ^{13}C]-glucose with the goal of distinguishing between glycolytic and pentose phosphate pathway (PPP) activity in rat 9L glioma cells [18]. In line with the current results, they found a 6 – 14% ^{2}H label loss in lactate originating from [6,6-$^{2}H_2$]-glucose. For [1-^{2}H]-glucose the ^{2}H label loss was much greater, likely due to phosphomannose isomerase activity [18]. Similar results were obtained by Funk et al. reporting minimal KIEs for [$^{2}H_7$]-glucose in glycolysis,

and for [$^{2}H_3$]-pyruvate in TCA cycle activity, studied in perfused rat heart [19,20]. Also the label loss reported by Funk et al. is in overall agreement with the data presented here [19,20].

When the ^{2}H label from [4-$^{2}H_x$]-glutamate re-enters the TCA cycle to complete the first turn, 50% of the ^{2}H label is lost in the conversion from succinate to fumarate. The symmetry of fumarate causes another 50% of the ^{2}H label to be lost during the conversion into malate and subsequently oxaloacetate. While the remaining ^{2}H label is incorporated into isocitrate at a position that ultimately corresponds to the C2 position in glutamate, the ^{2}H label never reaches glutamate as the label is removed in the conversion from isocitrate to α-ketoglutarate. Figure 5 shows the steady-state ^{2}H and ^{13}C label accumulation in downstream metabolic products of cerebral glucose metabolism. Following a 2-hour infusion of [6,6-$^{2}H_2$]-glucose, significant ^{2}H label accumulation is present in the H3 position of lactate and alanine and the H4 position of glutamate and glutamine (Fig. 5A). Small amounts of ^{2}H label accumulation can also be detected for the methyl group of *N*-acetyl aspartate (NAA, 2.01 ppm) and the H3 position of aspartate at circa 2.7 ppm. ^{2}H label accumulation in the glutamate/glutamine H3 position is noticeably missing. This is especially striking when compared to the amount of ^{13}C label accumulation in the C3 position of glutamate/glutamine (Fig. 5C/D). The lack of ^{2}H label accumulation can also be observed for GABA-H3 (1.89 ppm) and GABA-H4 (3.00 ppm). Spectral overlap with the intense signal from [6,6-$^{2}H_2$]-glucose at ~3.8 ppm, prevents the detection and assessment of ^{2}H label accumulation in the H2 position of glutamate/glutamine at ~3.75 ppm. A 2-hour infusion of [1-^{2}H]-glucose (Fig. 5B) eliminates the spectral overlap, thereby establishing the absence of ^{2}H label accumulation in the glutamate/glutamine H2 position. These experiments confirm the theoretically predicted absence of ^{2}H label at the C2 and C3 position of glutamate and glutamine.

The precision of the reported values for label loss and KIE is predominantly determined by the SNR of the NMR spectra. To increase the SNR for the analysis of glutamate and glutamine we pooled the samples of 5 animals, which is a limitation of this study. By using a Monte-Carlo analysis on the single data set we recovered the variability caused by the SNR of the NMR experiment, but pooling the sample sacrificed any insight into potential inter-subject variability. Several technical improvements could increase the NMR sensitivity and prevent the need to combine samples. Using a higher magnetic field spectrometer, smaller NMR tubes that require less sample dilution, and a cryo-cooled ^{13}C probe would all increase the ^{13}C NMR sensitivity, but were not readily available to us.

In conclusion, we quantified the ^{2}H label loss of [6,6-$^{2}H_2$]-glucose and [$^{2}H_3$]-acetate that occurs through metabolism in rat brain, and estimated the KIE. These data will be useful for quantitative studies aimed at mapping metabolic rates *in vivo* using these ^{2}H-labeled substrates with DMS and DMI techniques.

METHODS

Experimental design

The experimental design employed in the current study uses ^{13}C NMR spectroscopy during a co-administration experiment to follow the metabolic fate of both single-labeled ^{13}C and

double-labeled [^{2}H, ^{13}C] substrates [21]. Because the ^{13}C resides in the backbone of the metabolites, and therefore ^{13}C label is not lost, the total amount of double-^{13}C-labeled product equals the maximum amount of ^{13}C label that has flowed through the metabolic pathway of interest. The ^{13}C-^{13}C scalar coupling provides a doublet spectral pattern uniquely different from any pattern generated by [6,6-$^{2}H_2$, 6-^{13}C]-glucose. The ^{13}C label of [6,6-$^{2}H_2$, 6-^{13}C]-glucose will ultimately label [$^{2}H_x$, 3-^{13}C]-lactate, [$^{2}H_x$, 4-^{13}C]-glutamate and [$^{2}H_x$, 4-^{13}C]-glutamine with x = 0, 1 or 2. Metabolic products with both deuterons still attached (no ^{2}H label loss) will provide a unique quintet spectral pattern (1 : 2 : 3 : 2 : 1 intensity ratio) that in the ^{13}C NMR spectrum is shifted upfield by circa 0.5 – 0.6 ppm relative to the non-deuterated product [22,23]. In the presence of ^{2}H label loss, the single-deuterated products will generate a characteristic triplet pattern (1 : 1 : 1 intensity ratio) shifted upfield by circa 0.25 – 0.30 ppm. When all deuterons are lost, the non-deuterated form will resonate as a singlet, but still uniquely different from the non-deuterated doublet originating from the ^{13}C-^{13}C labeled substrate. The ^{2}H label loss can therefore be readily obtained by determining the relative amounts of non, single and double-deuterated products. If a significant ^{2}H KIE is present, the metabolic flow of ^{13}C label from the deuterated substrate will be slower than of the non-deuterated substrate.

In a separate study, the accumulation of ^{2}H label in downstream metabolic products was investigated at isotopic steady-state. For this purpose, animals were infused for 2 hours with [1-^{2}H]-glucose, [6,6-$^{2}H_2$]-glucose or [1-^{13}C]-glucose. Using direct ^{2}H NMR, the [6,6-$^{2}H_2$]-glucose study allows the detection of ^{2}H label accumulation in the H3 and H4 positions of glutamate and glutamine. Unfortunately, the strong [6,6-$^{2}H_2$]-glucose signal at ~3.8 ppm overlaps and thus obscures any ^{2}H label accumulation in the C2 position of glutamate or glutamine at ~ 3.75 ppm. Using [1-^{2}H]-glucose eliminates this spectral overlap, thereby allowing the measurement of steady-state ^{2}H label accumulation in the H2, H3 and H4 positions of glutamate and glutamine, albeit at a lower sensitivity than the [6,6-$^{2}H_2$]-glucose study. ^{13}C label accumulation from [1-^{13}C]-glucose as detected with ^{1}H-[^{13}C]-NMR was used as a ‘gold standard’ reference, because no ^{13}C-label is expected to be lost.

The KIE and ^{2}H label loss was also studied *in vitro* in rat glioma (RG2) cells. Similar to normal brain, glucose enters the glycolytic pathway after which the ^{2}H and ^{13}C labels end up in lactate. However, unlike normal brain the intracellular lactate that is exported from the cells accumulates linearly over time in the cell culture medium (Fig. S1A). The ^{2}H label loss can be quantitatively determined at the level of lactate from the unique spectral patterns of non (x=0), single (x=1) and double (x=2)-deuterated compounds, similar to that in rat brain (Fig. S1B). While the ability to measure kinetic isotope effects (KIEs) in rat brain is limited to early time points (Fig. 1B), the ability to measure KIEs in lactate produced by RG2 cancer cells improves over time as the extracellular lactate concentration (and thus the NMR sensitivity) increases over time. In the current study, KIEs on lactate were determined six hours after the co-administration of [6,6-$^{2}H_2$, 6-^{13}C] and [5,6-$^{13}C_2$]-labeled glucose.

RG2 cell medium studies

RG2 cells were purchased from American Type Culture Collection (ATCC) Cells were grown in 75 cm^{2} flasks at 37°C in humidified air and 5% CO_2 in Dulbecco’s modified

Eagle's medium (DMEM; Gibco), supplemented with 10% heat-inactivated fetal bovine serum (Gibco) and 1% penicillin streptomycin (Gibco). RG2 cell experiments were performed in 3 cell flasks each containing 6 to 8 million cells. The standard cell culture medium was replaced with 10 ml of medium containing 1 M of [5,6-$^{13}C_2$]-glucose and 1 M of [6,6-$^{2}H_2$, 6-^{13}C]-glucose. After six hours of incubation the medium was collected, lyophilized (LabConco, Kansas City, MO, USA), and resuspended in 600 μL of phosphate-buffered (100 mM, pH 7.2) D_2O/H_2O (10/90%) solution, containing 3 mM formate (for ^{1}H NMR chemical shift referencing), and 3 mM imidazole (for pH determination).

In vivo rat studies

All procedures on animals were performed under approved protocols by the Yale Animal Care and Use Committee in accordance with American Veterinary Medical Association (AVMA) guidelines on euthanasia.

Male Fischer 344 rats, body weight (BW) 220 ± 30 g (mean ± SD) were anaesthetized with isoflurane (3.5% for induction, 1.5 – 1.8% for maintenance) in 70%/30% N_2O/O_2 via a nose cone. Non-fasted animals (n = 5) received an intravenous co-infusion of equimolar (0.5 M) [5,6-$^{13}C_2$]-glucose and [6,6'-$^{2}H_2$, 6-^{13}C]-glucose through a catheter placed in the tail vein. Briefly, animals received an initial bolus (135 μL per 100 g body weight) followed by a continuous intravenous infusion of the glucose infusate. The infusion rate was decreased every 30 s according to a decreasing exponential function during the first 8 min and was constant at 6.85 μL/min/100g BW for the remainder of the experiment. The total infusion duration was 20 min, representing a balance between the attainable signal-to-nose ratio (SNR) and sensitivity towards KIEs. Another group of 5 non-fasted rats similarly received an intravenous infusion of equimolar [1,2-$^{13}C_2$]-acetate and [$^{2}H_3$, 2-^{13}C]-acetate. After an initial bolus of 40 μL/100 g BW, acetate was infused at decreasing rates (2 steps) before settling at a constant rate of 12.5 μL/min/100 g BW 4 min after the bolus administration. Following 20 min of infusion, animals were euthanized by focused-beam microwave irradiation (4.5 kW for 0.9 s, Muromachi Microwave Fixation System, Stoelting Co, Wood Dale, IL, USA), instantly stopping enzyme activity and cerebral metabolism. An additional four Fischer rats were euthanized without substrate infusion in order to establish ^{13}C natural abundance signal intensities. Following microwave irradiation, the rat head was decapitated, and the brain dissected. After weighing rat brain tissue (1.32 ± 0.15 g), a known amount of [2-^{13}C]-glycine was added as concentration standard, and the samples homogenized using a bead mill (Omni International, Kennesaw GA, USA), in a 0.1 M HCl/methanol (2:1 vol/wt) solution, followed by extraction with ethanol. The supernatant was clarified by centrifugation, lyophilized and resuspended in 600 μL of the buffer described above (RG2 cell medium studies).

For glucose infusion studies NMR data were acquired from each brain sample preparation and used to analyze KIE and label loss in lactate. Next, to increase the signal-to-noise ratio (SNR) these samples were dried and resuspended as one sample before NMR data were acquired for analysis of KIE and label loss in glutamate and glutamine. For the acetate study, brain samples were pooled as well.

In a separate study, animals (n = 2 per substrate) received an intravenous infusion of 0.75 or 1 M of [1-^{2}H]-glucose, [6,6-$^{2}H_2$]-glucose or [1-^{13}C]-glucose for 2 hours according to the protocol described above. At the end of the infusion, animals were euthanized by focused-beam microwave irradiation. Brain tissue processing and NMR sample preparation were performed as described above. Except for the analysis of steady-state ^{2}H label accumulation, for which the phosphate-buffered NMR solution was based on ^{2}H-depleted water, and did not contain D_2O or [2-^{13}C]-glycine. Steady-state ^{2}H and ^{13}C label accumulation were determined by direct ^{2}H NMR and indirect ^{1}H-[^{13}C]-NMR, respectively.

NMR spectroscopy

All experiments were performed on a Bruker Avance spectrometer (Bruker Instruments, Billerica, MA, USA) operating at 500.13 MHz for ^{1}H and equipped with a 5-mm broadband (BB) probe incorporating a single-axis (Z) gradient coil. The magnetic field homogeneity on each sample was optimized with an automated 1D field mapping algorithm capable of adjusting up to fifth order zonal spherical harmonics.

Direct ^{13}C-[^{1}H] NMR spectra were acquired with a pulse-acquire method (TR = 20 s) as 16,384 complex points over a 25.2 kHz (or 200 ppm) spectral width. For a select number of studies, the repetition time was lengthened to 180 s to accommodate the long T_1 relaxation times of non-protonated carbons, such as [2-$^{3}H_2$, 2-^{13}C]-acetate. Broadband adiabatic ^{1}H decoupling was applied during the total acquisition time of 650 ms. The decoupling sequence was executed with 2.0 ms AFP pulses [HS8 modulation [24], $\Delta\nu_{max}$ = 10 kHz, B_{2max} = 2.5 kHz, center frequency = 3.5 ppm) incorporated in a 20-step supercycle [25]. In order to avoid selective enhancement of protonated over deuterated carbon positions, nuclear Overhauser enhancement was omitted in all studies.

Direct ^{2}H NMR spectra were acquired at 76.77 MHz with a pulse-acquire method (TR = 2 s) as 4,096 complex points over a 5.0 kHz spectral width. Indirect ^{1}H-[^{13}C] NMR or Proton-Observed, Carbon-Edited (POCE) NMR spectra were acquired with an adiabatic spin-echo sequence employing 1 ms BIR-4 pulses for excitation and refocusing (tanh/tan modulation [26], pulse length, T = 1.0 ms, maximum frequency sweep, $\Delta\nu_{max}$ = 100 kHz, maximum RF amplitude, B_{1max} = 10 kHz, TR = 25 s, TE = 8 ms). On alternate scans an adiabatic full passage inversion pulse (HS8 modulation, T = 1.0 ms, $\Delta\nu_{max}$ = 20 kHz, B_{2max} = 10 kHz, [24]) was executed on the carbon-13 channel (125.76 MHz) at the same time as the proton refocusing pulse. Broadband adiabatic ^{13}C decoupling was applied during the total acquisition time. The decoupling sequence was executed with 2.0 ms AFP pulses (HS8 modulation, $\Delta\nu_{max}$ = 10 kHz, B_{2max} = 2.5 kHz, center frequency = 34.2 ppm) incorporated in a 20-step supercycle [25]. Water suppression was achieved with a six-pulse CHESS (chemical shift selective, [27]) sequence executed with 10 ms Gaussian pulses truncated at 10% of the maximum amplitude.

Data processing

All ^{13}C MR spectra were quantified with home-written Matlab (Matlab 8.0, The Mathworks, Natick, MA, USA) spectral fitting software using ^{13}C chemical shifts and ^{2}H-^{13}C scalar couplings determined from the measured data and summarized in Table S1. The glucose

infusate ^{2}H MR spectra were modeled with three contributions related to the double ^{13}C-labeled and non and double-deuterated forms. The acetate infusate ^{2}H NMR spectra were modeled with three contributions related to the double-carbonated and non and triple-deuterated forms. Impurities from single-deuterated glucose or single/double-deuterated acetate were not observed. Lactate, glutamate and glutamine signals were modeled with basis sets containing four contributions related to the double ^{13}C-labeled and non, single and double-deuterated forms. The overall glutamate spectral fit was improved by the addition of contributions from labeling patterns expected for glutamate ^{13}C-labeled in the second turn of the TCA cycle. The resonance line widths, chemical shifts and phases for all components were constrained to 0.5 – 3.0 Hz, ± 1.0 Hz and ± 5.0°, respectively. The overall spectral fit was completed with a low-order (constant or linear) spectral baseline.

The natural abundance contribution to the non-deuterated glutamate and glutamine signals was established using the ^{13}C MR spectra obtained from rat brain tissue of animals without substrate infusion. The natural abundance NAA signal at 22.8 ppm was used to account for small inter-sample differences related to tissue amounts and RF coil efficiency. The natural abundance contribution to the non-deuterated [3-^{13}C]-lactate signal was established by comparison with the non-labeled [2-^{13}C]-lactate signal at 69.3 ppm.

Statistics

The effect of label loss is analyzed by descriptive statistics (mean and standard deviation, SD), as presented in Figs 2-5. The potential KIE in RG2 cells was analyzed by comparing the NMR signal amplitude of lactate labeled by [6,6-$^{2}H_2$, 6-^{13}C]-glucose with lactate generated from non-deuterated [5,6-$^{13}C_2$]-glucose, using the non-parametric Wilcoxon Signed Rank test (because of the small sample size of n = 3). The potential KIE in brain was analyzed by comparing the NMR signal amplitude of lactate labeled by [6,6-$^{2}H_2$, 6-^{13}C]-glucose (n = 5) with the signal amplitude of lactate generated from non-deuterated [5,6-$^{13}C_2$]-glucose, using the paired sample T-test. Brain samples from 5 animals were pooled to increase the SNR for detection of ^{2}H and ^{13}C-labeled glutamate and glutamine. A Monte Carlo analysis was performed to generate 20 datasets based on the NMR spectrum of the pooled sample. These 20 datasets were individually quantified. This approach was used for both the glucose and acetate studies, and the potential KIE was analyzed by comparing the signal amplitude of metabolites labeled by the deuterated substrate with those from non-deuterated substrates using the paired sample T-test.

Supplementary Material

Refer to Web version on PubMed Central for supplementary material.

ACKNOWLEDGMENTS

The authors thank Xiaoxian Ma for his assistance with animal preparation. This research was funded, in part, by NIH grants NIMH R01-MH095104, NIBIB R01-EB025840, and a research grant program from Cambridge Isotope Laboratories.

REFERENCES

(1). Rothman DL; Graaf RA de; Hyder F; Mason GF; Behar KL; Feyter HMD. In Vivo 13C and 1H-[13C] MRS Studies of Neuroenergetics and Neurotransmitter Cycling, Applications to Neurological and Psychiatric Disease and Brain Cancer. NMR Biomed 2019, 32 (10), e4172. 10.1002/nbm.4172. [PubMed: 31478594]

(2). Ven K. C. C. van de; Tack CJ; Heerschap A; van der Graaf, M.; Galan B. E. de. Patients with Type 1 Diabetes Exhibit Altered Cerebral Metabolism during Hypoglycemia. J. Clin. Invest 2013, 123 (2), 623–629. 10.1172/JCI62742. [PubMed: 23298837]

(3). Buehler T; Bally L; Dokumaci AS; Stettler C; Boesch C Methodological and Physiological Test–Retest Reliability of 13C-MRS Glycogen Measurements in Liver and in Skeletal Muscle of Patients with Type 1 Diabetes and Matched Healthy Controls. NMR Biomed 2016, 29 (6), 796–805. 10.1002/nbm.3531. [PubMed: 27074205]

(4). Shulman GI; Rothman DL; Jue T; Stein P; DeFronzo RA; Shulman RG Quantitation of Muscle Glycogen Synthesis in Normal Subjects and Subjects with Non-Insulin-Dependent Diabetes by 13C Nuclear Magnetic Resonance Spectroscopy. N. Engl. J. Med 1990, 322 (4), 223–228. 10.1056/NEJM199001253220403. [PubMed: 2403659]

(5). De Feyter HM; Behar KL; Rao JU; Madden-Hennessey K; Ip KL; Hyder F; Drewes LR; Geschwind J-F; Graaf R. A. de; Rothman DL. A Ketogenic Diet Increases Transport and Oxidation of Ketone Bodies in RG2 and 9L Gliomas without Affecting Tumor Growth. Neuro-Oncol 2016, 18 (8), 1079–1087. 10.1093/neuonc/now088. [PubMed: 27142056]

(6). Wijnen JP; Van der Graaf M; Scheenen TWJ; Klomp DWJ; de Galan BE; Idema AJS; Heerschap A In Vivo 13C Magnetic Resonance Spectroscopy of a Human Brain Tumor after Application of 13C-1-Enriched Glucose. Magn. Reson. Imaging 2010, 28 (5), 690–697. 10.1016/j.mri.2010.03.006. [PubMed: 20399584]

(7). Terpstra M; Gruetter R; High WB; Mescher M; DelaBarre L; Merkle H; Garwood M Lactate Turnover in Rat Glioma Measured by in Vivo Nuclear Magnetic Resonance Spectroscopy. Cancer Res 1998, 58 (22), 5083–5088. [PubMed: 9823316]

(8). Rodrigues TB; Serrao EM; Kennedy BWC; Hu D-E; Kettunen MI; Brindle KM Magnetic Resonance Imaging of Tumor Glycolysis Using Hyperpolarized 13C-Labeled Glucose. Nat. Med 2014, 20 (1), 93–97. 10.1038/nm.3416. [PubMed: 24317119]

(9). Mishkovsky M; Anderson B; Karlsson M; Lerche MH; Sherry AD; Gruetter R; Kovacs Z; Comment A Measuring Glucose Cerebral Metabolism in the Healthy Mouse Using Hyperpolarized 13 C Magnetic Resonance. Sci. Rep 2017, 7 (1), 11719. 10.1038/s41598-017-12086-z. [PubMed: 28916775]

(10). Ming Lu; Xiao-Hong Zhu; Yi Zhang; Gheorghe Mateescu; Wei Chen. Quantitative Assessment of Brain Glucose Metabolic Rates Using in Vivo Deuterium Magnetic Resonance Spectroscopy. J. Cereb. Blood Flow Metab 2017, 37 (11), 3518–3530. 10.1177/0271678X17706444. [PubMed: 28503999]

(11). De Feyter HM; Behar KL; Corbin ZA; Fulbright RK; Brown PB; McIntyre S; Nixon TW; Rothman DL; de Graaf RA Deuterium Metabolic Imaging (DMI) for MRI-Based 3D Mapping of Metabolism in Vivo. Sci. Adv 2018, 4 (8), eaat7314. 10.1126/sciadv.aat7314. [PubMed: 30140744]

(12). de Graaf RA; Hendriks AD; Klomp DWJ; Kumaragamage C; Welting D; Castro C. S. A. de; Brown PB; McIntyre S; Nixon TW; Prompers JJ; De Feyter HM. On the Magnetic Field Dependence of Deuterium Metabolic Imaging. NMR Biomed 2020, 33 (3), e4235. 10.1002/nbm.4235. [PubMed: 31879985]

(13). Westheimer FH The Magnitude of the Primary Kinetic Isotope Effect for Compounds of Hydrogen and Deuterium. Chem. Rev 1961, 61 (3), 265–273. 10.1021/cr60211a004.

(14). Thomson JF; Alexander P Biological Effects of Deuterium; Macmillan, 1963.

(15). Murphy RB; Wyatt NA; Fraser BH; Yepuri NR; Holden PJ; Wotherspoon ATL; Darwish TA A Rapid MS/MS Method to Assess the Deuterium Kinetic Isotope Effect and Associated Improvement in the Metabolic Stability of Deuterated Biological and Pharmacological Molecules as Applied to an Imaging Agent. Anal. Chim. Acta 2019, 1064, 65–70. 10.1016/j.aca.2019.02.025. [PubMed: 30982519]

(16). Cooper AJ Proton Magnetic Resonance Studies of Glutamate-Alanine Transaminase-Catalyzed Deuterium Exchange. Evidence for Proton Conservation during Prototropic Transfer from the Alpha Carbon of L-Alanine to the C4-Position of Pyridoxal 5'-Phosphate. J. Biol. Chem 1976, 251 (4), 1088–1096. [PubMed: 1249068]

(17). Malloy CR; Sherry AD; Jeffrey FM Analysis of Tricarboxylic Acid Cycle of the Heart Using 13C Isotope Isomers. Am. J. Physiol.: Heart Circ. Physiol 1990, 259 (3), H987–H995.

(18). Ben-Yoseph O; Kingsley PB; Ross BD Metabolic Loss of Deuterium from Isotopically Labeled Glucose. Magn. Reson. Med 1994, 32 (3), 405–409. [PubMed: 7984074]

(19). Funk AM; Anderson BL; Wen X; Hever T; Khemtong C; Kovacs Z; Sherry AD; Malloy CR The Rate of Lactate Production from Glucose in Hearts Is Not Altered by Per-Deuteration of Glucose. J. Magn. Reson 2017, 284, 86–93. 10.1016/j.jmr.2017.09.007. [PubMed: 28972888]

(20). Funk AM; Wen X; Hever T; Maptue NR; Khemtong C; Sherry AD; Malloy CR Effects of Deuteration on Transamination and Oxidation of Hyperpolarized 13C-Pyruvate in the Isolated Heart. J. Magn. Reson 2019, 301, 102–108. 10.1016/j.jmr.2019.03.003. [PubMed: 30861456]

(21). Mason RP; Sanders JKM; Cornish AC Approaching Enzymic Kinetic Isotope Effects in Vivo by Nuclear-Magnetic-Resonance Spectroscopy. Biochem. Soc. Trans 1987, 15 (1), 148–149. 10.1042/bst0150148.

(22). Gutowsky HS Isotope Effects in High Resolution NMR Spectroscopy. J. Chem. Phys 1959, 31 (6), 1683–1684. 10.1063/1.1730682.

(23). Mantsch HH; Saitô H; Smith ICP Deuterium Magnetic Resonance, Applications in Chemistry, Physics and Biology. Prog. Nucl. Magn. Reson. Spectrosc 1977, 11 (4), 211–272. 10.1016/0079-6565(77)80010-1.

(24). Tannús A; Garwood M Improved Performance of Frequency-Swept Pulses Using Offset-Independent Adiabaticity. J. Magn. Reson., Ser. A 1996, 120 (1), 133–137. 10.1006/jmra.1996.0110.

(25). Fujiwara T; Nagayama K Composite Inversion Pulses with Frequency Switching and Their Application to Broadband Decoupling. J. Magn. Reson 1988, 77 (1), 53–63. 10.1016/0022-2364(88)90031-5.

(26). Garwood M; Ke Y Symmetric Pulses to Induce Arbitrary Flip Angles with Compensation for Rf Inhomogeneity and Resonance Offsets. J. Magn. Reson 1991, 94 (3), 511–525. 10.1016/0022-2364(91)90137-I.

(27). Haase A; Frahm J; Hanicke W; Matthaei D 1 H NMR Chemical Shift Selective (CHESS) Imaging. Phys. Med. Biol 1985, 30 (4), 341–344. 10.1088/0031-9155/30/4/008. [PubMed: 4001160]

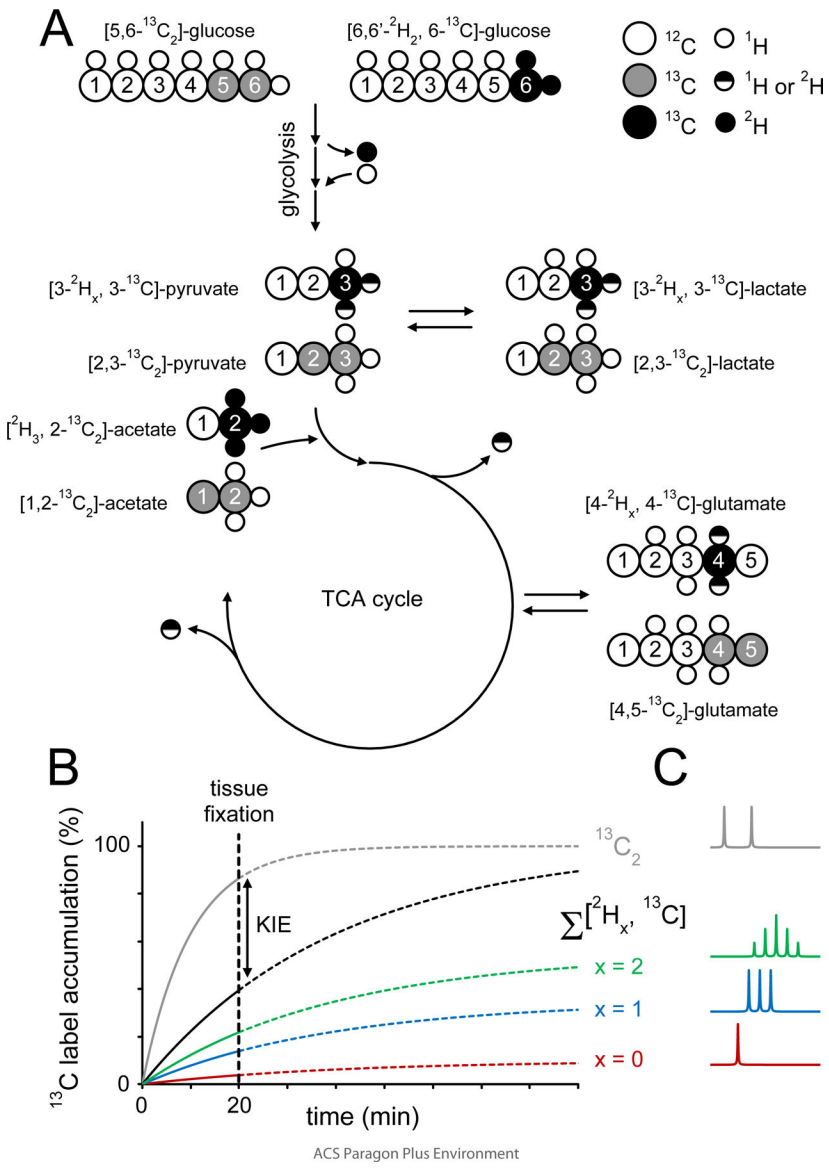

Figure 1–.

Illustration of the strategy used to detect deuterium label loss and kinetic isotope effects during cerebral acetate and glucose metabolism. The metabolic fate of [6,6-$^{2}H_2$, 6-^{13}C]-glucose or [$^{2}H_3$, 2-^{13}C]-acetate and the amount of deuterium label loss can be studied with ^{13}C MRS, whereby different chemical shifts and scalar coupling patterns allow the distinction between non, single and double-deuterated metabolic products. Glucose undergoes glycolysis where the ^{2}H and ^{13}C labels end up in the methyl groups of pyruvate and lactate. The glycolytic pathway provides several opportunities for $^{1}H/^{2}H$ label exchange, such that the ^{2}H amount on pyruvate and lactate will be reduced relative to glucose. Pyruvate will, via conversion to acetyl-CoA, enter the tricarboxylic acid (TCA) cycle where the ^{2}H and ^{13}C isotopes will label the glutamate, glutamine and GABA pools. Several TCA cycle reactions lead to removal or replacement of ^{2}H, thus further reducing the amount of ^{2}H in downstream metabolic products such as glutamate. Whereas

the ^{2}H label loss can be quantitatively determined from the unique spectral patterns of non, single and double-deuterated compounds, the study does not provide information on ^{2}H-induced kinetic isotope effects. Kinetic isotope effects were determined by comparing the total label flow from [6,6-$^{2}H_2$, 6-^{13}C]-glucose (and [$^{2}H_3$, 2-^{13}C]-acetate) with that of non-deuterated [5,6-$^{13}C_2$]-glucose ([1,2-$^{13}C_2$]-acetate), whereby the ^{13}C-^{13}C scalar coupling provided unique spectral patterns different from those originating from [6,6-$^{2}H_2$, 6-^{13}C]-glucose ([$^{2}H_3$, 2-^{13}C]-acetate). (B) Isotopic label accumulation curves for an (unspecified) metabolic product in the presence of a significant KIE. The individual non-deuterated (x = 0), single-deuterated (x = 1) and double-deuterated (x = 2) metabolic products provide a quantitative evaluation of ^{2}H label loss. A comparison between the sum of all three ^{13}C-labeled (Σx) products and the $^{13}C_2$-labeled product gives a quantitative evaluation of a ^{2}H-mediated KIE. A single-point measurement was made at 20 min following the onset of intravenous infusion (dotted vertical line). The selected time point represents a compromise between the attainable NMR sensitivity and the ability to accurately detect label loss and kinetic isotope effects. (C) Examples of ^{1}H-decoupled ^{13}C NMR spectra form metabolites with 13C and ^{13}C + ^{2}H label as indicated in (B). Note the spectral pattern as a function of number (x) of ^{2}H's attached to ^{13}C. x = 0 has no coupling effect, x = 1 leads to a 1 : 1 : 1 triplet intensity ratio, x = 2 leads to 1 : 2 : 3 : 2 : 1 quintet intensity ratio. See also Table S1 for more detail on coupling constants and spectral patterns.

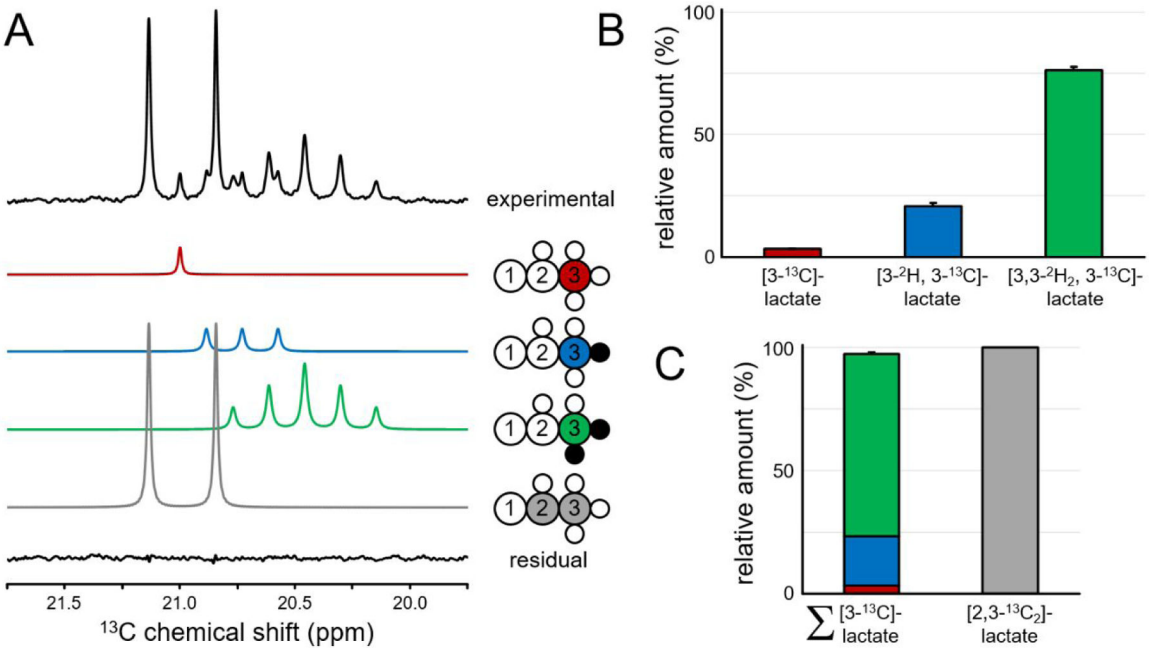

Figure 2–.

^{2}H and ^{13}C label incorporation in lactate produced by RG2 cells. (A) ^{13}C NMR spectrum from RG2 cell medium showing four different $^{2}H/^{13}C$-labeled lactate species originating from two glucose substrates, [5,6-$^{13}C_2$]-glucose and [6,6-$^{2}H_2$, 6-^{13}C]-glucose. The four lactate species and their fitted spectral contributions are color-coded as indicated. The bottom trace shows the difference between the experimental data (top trace) and the sum of the four fitted contributions. Small open white and closed black circles indicate protons and deuterons, respectively. (B) ^{2}H label distribution for lactate produced from [6,6-$^{2}H_2$, 6-^{13}C]-glucose. Lactate species containing zero, one and two deuterons account for 3.2 ± 0.3 %, 20.7 ± 1.2 % and 76.1 ± 1.4 % of all lactate originating from [6,6-$^{2}H_2$, 6-^{13}C]-glucose, respectively. The ^{2}H label loss for lactate therefore amounts to 13.6 % of the theoretical maximum ^{2}H label accumulation (two deuterons on every lactate). (C) Lactate production from [6,6-$^{2}H_2$, 6-^{13}C]-glucose (left) amounts to 97.3 ± 0.9 % of that originating from [5,6-$^{13}C_2$]-glucose (right).

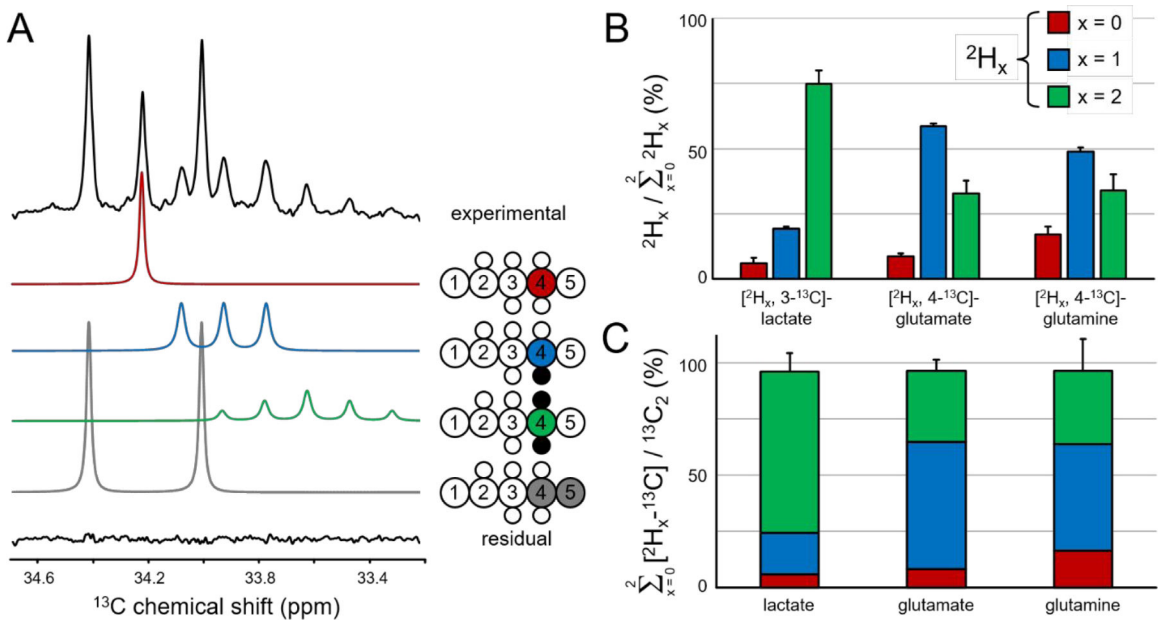

Figure 3–.

Deuterium label loss and kinetic isotope effect for lactate, glutamate and glutamine in rat brain following 20 min of intravenous infusion of [6,6-$^{2}H_2$, 6-^{13}C]-glucose and [5,6-$^{13}C_2$]-glucose. (A) Experimental ^{13}C NMR spectrum (top) for [4-^{13}C]-glutamate together with the fitted contributions from non-deuterated [4-^{13}C]-glutamate (red), single-deuterated [4-^{2}H, 4-^{13}C]-glutamate (blue), double-deuterated [4,4-$^{2}H_2$, 4-^{13}C]-glutamate (green) and non-deuterated [4, 5-$^{13}C_2$]-glutamate (gray). The residual between the experimental and total fitted spectra is shown as the bottom trace. (B) Deuterium label loss for [3-^{13}C]-lactate, [4-^{13}C]-glutamate and [4-^{13}C]-glutamine originating from [6,6-$^{2}H_2$,6-^{13}C]-glucose. Non, single and double-deuterated compounds are indicated by red, blue and green bars, respectively. For each compound the sum of the three contributions equals 100%. (C) Kinetic isotope effect for lactate, glutamate and glutamine. The absolute amounts of non, single and deuterated compounds are added together and compared to the absolute amount of [2,3-$^{13}C_2$]-lactate or [4,5-$^{13}C_2$]-glutamate or glutamine which is defined as 100%.

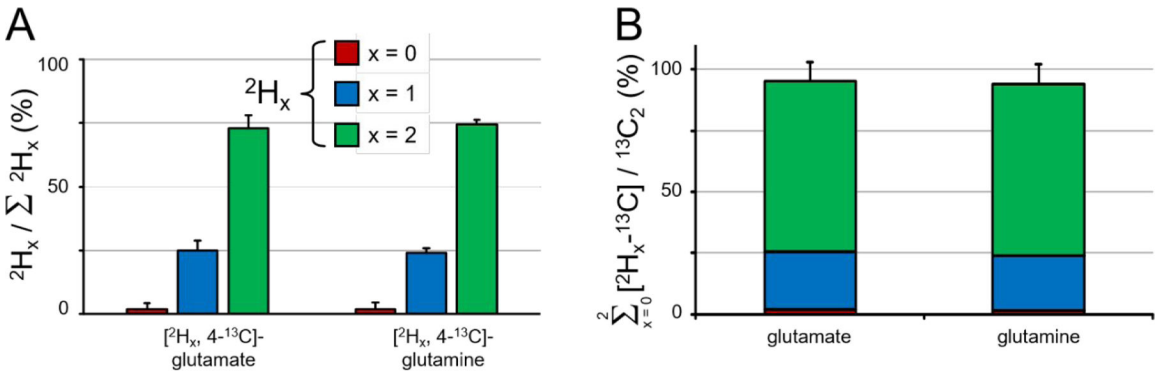

Figure 4–.

Deuterium label loss and kinetic isotope effect for glutamate and glutamine in rat brain following 20 min of intravenous infusion of [$^2H_3$, 2-^{13}C]-acetate and [1,2-$^{13}C_2$]-acetate. (A) Deuterium label loss for [4-^{13}C]-glutamate and [4-^{13}C]-glutamine originating from [$^2H_3$, 2-^{13}C]-acetate. Non, single and double-deuterated compounds are indicated by red, blue and green bars, respectively. For each compound the sum of the three contributions equals 100%. (B) Kinetic isotope effect for glutamate and glutamine. The absolute amounts of non, single and deuterated compounds are added together and compared to the absolute amount of [4,5-$^{13}C_2$]-glutamate or glutamine which is defined as 100%. Error bars based on Monte Carlo simulation of n = 20.

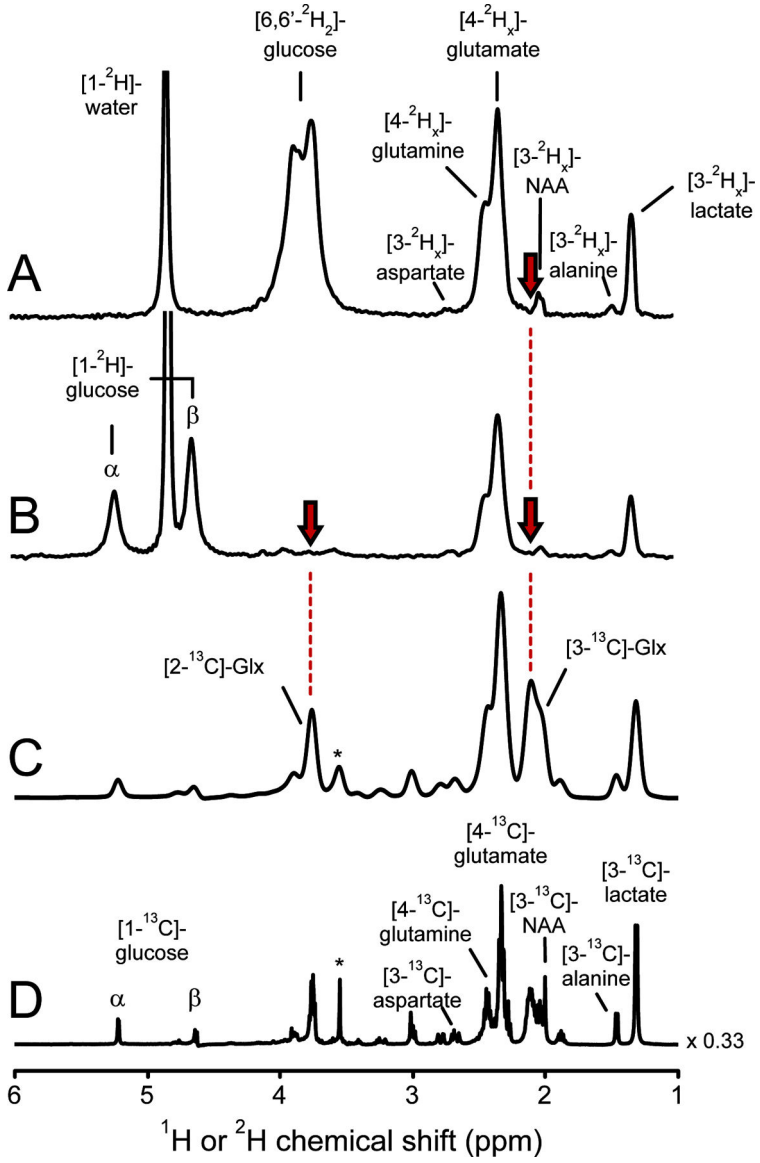

Figure 5–.

Steady-state ^{2}H or ^{13}C label accumulation in rat brain following intravenous infusion of ^{2}H or ^{13}C-labeled glucose. (A, B) ^{2}H NMR spectra from rat brain extract following 2 hours of intravenous (A) [6,6-$^{2}H_2$]-glucose or (B) [1-^{2}H]-glucose infusion. (C, D) ^{1}H-[^{13}C] (POCE) NMR difference spectra following 2 hours of intravenous [1-^{13}C]-glucose infusion. Spectrum (C) is identical to (D) with the exception of an additional 25 Hz Lorentzian line broadening to approximate the ^{2}H line widths in (A, B). Due to ^{2}H label loss the x index lays in the range $0 \leq x \leq 2$ and $0 \leq x \leq 1$ for all downstream products of (A) [6,6-$^{2}H_2$]-glucose and (B) [1-^{2}H]-glucose, respectively. (A) ^{2}H label accumulation in the C3 position of glutamate and glutamine (red arrow) is noticeably missing ($x \sim 0$), in stark contrast to significant ^{13}C label accumulation (C). ^{2}H label accumulation in the C2 position of glutamate and glutamine cannot be determined in (A) due to severe spectral overlap with [6,6-$^{2}H_2$]-glucose. (B) A [1-^{2}H]-glucose infusion eliminates the spectral overlap and

demonstrates the lack of ^{2}H label accumulation ($x \sim 0$) in the C2 position of glutamate and glutamine (red arrow). Glx = glutamate + glutamine. The signal in (C, D) indicated with * originates from [2-^{13}C]-glycine, a chemical shift and concentration reference. NA: N-Acetyl aspartate.